Detection of Hotspots in Photovoltaic Modules of a Solar Power Plant through Dissimilarity Measurement of Thermal Images Acquired by Drone

Michel Santana Teodoro[1], João Roberto dos Santos Neto[1] and Douglas Bressan Riffel[1]

[1] Universidade Federal de Sergipe (UFS), São Cristóvão (Brazil)

Abstract

Early identification of thermal anomalies, such as hotspots, is essential to ensure the efficiency and longevity of photovoltaic systems. This work presents a methodology based on aerial inspection using a drone and quantitative analysis of thermal images for hotspot detection in photovoltaic modules. The approach combines module segmentation, projective correction, extraction of temperature matrices through the *DJI Thermal SDK*, and the application of dissimilarity metrics — *sum of absolute differences* and *sum of squared differences*. The inspections were carried out at a 1 MWp solar power plant located in the State of Sergipe, Brazil, with thermal data acquisition performed in accordance with IEC TS 62446-3:2017. The results show that the applied metrics effectively distinguish modules with and without hotspots, even under controlled induced-shading conditions. The proposed methodology demonstrated technical feasibility for fast, safe, and accurate inspections, contributing to predictive maintenance in large-scale photovoltaic systems. This study reinforces the role of aerial thermography as a strategic tool for the efficient and sustainable operation of solar power plants.

Keywords: Photovoltaic modules, drone thermography, hotspots, thermal dissimilarity, predictive maintenance.

1. Introduction

The growing adoption of photovoltaic systems for power generation has driven the need for effective techniques for monitoring and maintaining these installations. In particular, the early identification of failures such as hotspots is essential to ensure the efficiency, safety, and service life of photovoltaic modules, as well as to prevent significant energy losses.

Hotspots are localized regions within photovoltaic modules where excessive heating occurs due to electrical defects, shading, material degradation, or imperfect connections. These hotspots can be effectively identified through the analysis of thermal images. Previous studies have demonstrated that infrared thermography applied to photovoltaic modules is a reliable method for detecting abnormal heating patterns, particularly under partial shading conditions (Ikejiofor et al., 2020). When implemented with drones equipped with thermal cameras, this technique has proven to be a non-invasive, rapid, and accurate approach for large-scale inspection of solar power plants.

In the context of thermographic monitoring, accurate segmentation of photovoltaic modules and quantitative analysis of thermal variations are essential steps for the reliable detection of anomalies. Mathematical metrics such as the Sum of Absolute Differences (SAD) and the squared Euclidean distance — also known as the Sum of Squared Differences (SSD) — provide quantitative means to compare temperature matrices across different modules, aiding in the identification of modules exhibiting anomalous thermal behavior.

This study presents a methodology that combines drone-based thermal image acquisition, module segmentation with projective correction, and the application of SAD and SSD metrics to assess the presence of hotspots in a 1 MWp photovoltaic solar power plant located in the State of Sergipe, Brazil. Furthermore, the study follows standard recommendations for data acquisition and module emissivity determination, ensuring the accuracy and reliability of the thermal analyses.

10.18086/swc.2025.03.19 Available at http://proceedings.ises.org

2. Materials and methods

2.1. Power plant location and photovoltaic system characteristics

The study was conducted at a photovoltaic solar power plant with an installed capacity of 1 MWp (Figure 1), located in Carmópolis, a municipality in the eastern region of the State of Sergipe, Brazil. The plant consists of 2,344 photovoltaic modules measuring 2,008 × 1,002 × 40 mm, model JKM400M-72H-V from the Cheetah HC 72M series, manufactured by JinKO Solar, arranged in arrays connected to string inverters.

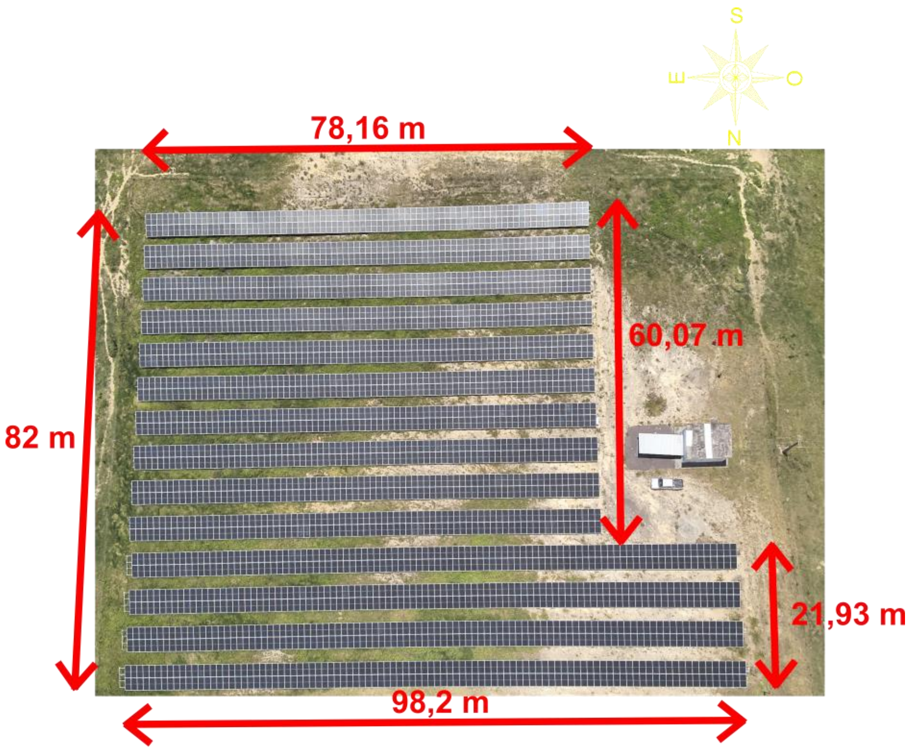

Figure 1: Aerial view of the 1 MWp photovoltaic solar plant used for image acquisition.

The photovoltaic modules are oriented toward true north with a tilt angle of 12° and no solar tracking. Each module consists of 144 (6 × 24) monocrystalline half-cells, with individual cell dimensions of 158.75 × 158.75 mm.

The selection of this power plant was based on the ease of access for aerial inspections using drones, enabling the capture of images under controlled and safe conditions.

2.2. Thermal image acquisition using drone

Thermal image acquisition was performed using a DJI Mavic 3T multirotor drone (Figure 2) from the DJI Mavic 3 Enterprise series, equipped with a thermal camera with a spectral response in the 8−14 µm range, a resolution of 640 × 512 pixels, and an optical system with a Diagonal Field of View (DFoV) of 61°.

Figure 2: DJI Mavic 3T drone.

The flights were conducted on clear-sky days at selected times to ensure solar irradiance above 600 W/m², in accordance with the Technical Specification (TS) 62446-3:2017 from the International Electrotechnical Commission (IEC), which regulates thermographic inspection of photovoltaic systems. According to this standard, all photovoltaic modules — including those observed at unfavorable angles of up to 30° — must be imaged with a minimum resolution of 5 × 5 pixels per photovoltaic cell (IEC, 2017).

To ensure compliance with this requirement, it was necessary to relate the angle α_d (camera DFoV) to the distance p between the lens and the photovoltaic panel, the camera resolution ($h \times w$, in pixels), and the Lateral Size of the Photovoltaic Module Cells ($LSPMC$). Figure 3 presents the geometric model adopted for this analysis, representing the scenario of thermal image capture by the drone.

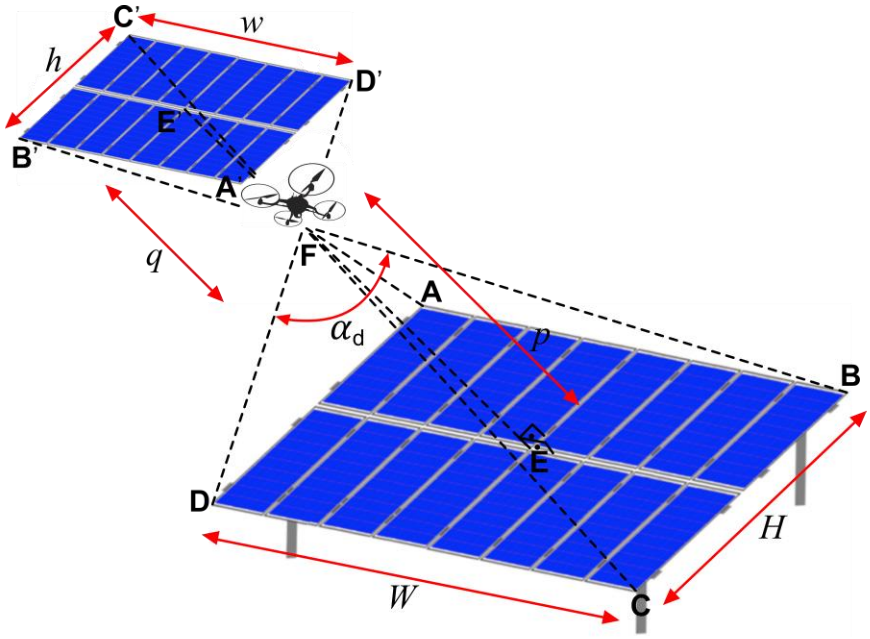

Figure 3: Geometric model for determining the distance between the thermographic lens and the photovoltaic panel.

The parameters involved allowed, through equation 1, the calculation of the maximum distance between the thermal camera lens and the photovoltaic panel that ensures the recommended minimum resolution of 5 × 5 pixels per cell.

$$p \leq \frac{LSPMC \cdot \sqrt{h^2 + w^2}}{10 \cdot \tan\left(\frac{\alpha_d}{2}\right)} \quad \text{(eq. 1)}$$

Once the maximum distance (22 m) was calculated, the drone was positioned to fly at 16.3 m from each photovoltaic panel, allowing approximately 28 modules to be captured per thermal image. Figure 4 shows the framing adopted during the aerial inspections.

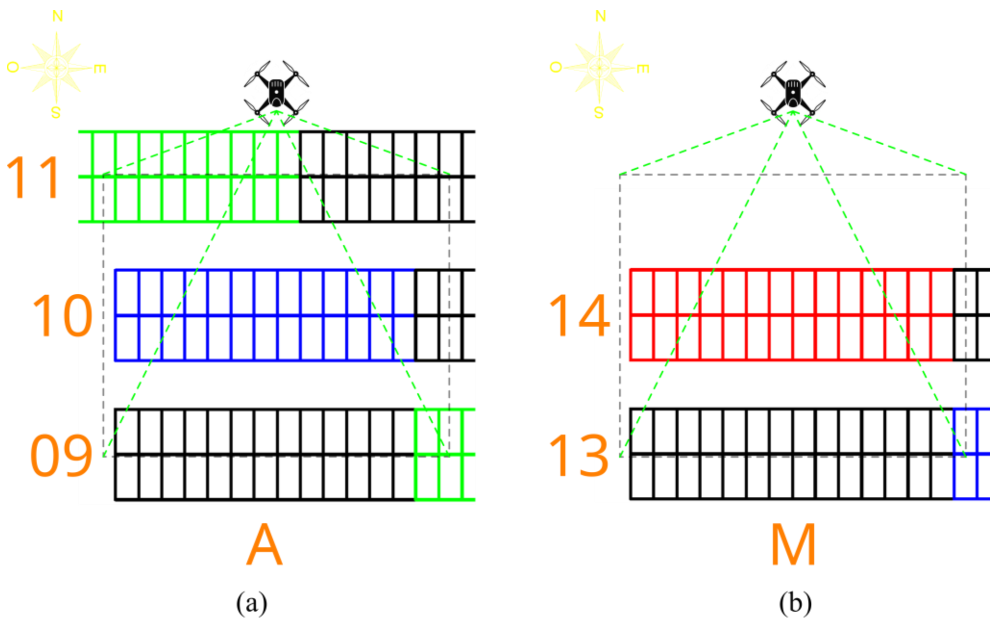

Figure 4: Framings adopted for the acquisition of thermal images of photovoltaic panels at the solar power plant: (a) panel A10; (b) panel M14.

2.3. Segmentation of individual photovoltaic modules from panels captured in thermal images

The thermal images captured were initially subjected to an edge detection process. As proposed by Zhang et al. (2017), the Canny edge detector was adopted, demonstrating high effectiveness in highlighting the contours of the photovoltaic modules in the drone-acquired images.

In the next step, the sides of each photovoltaic module were identified from the edge images. For this purpose, the version of the Hough transform attributed to Duda and Hart (1972) was employed, a technique that allows the detection of straight lines even in images with moderate noise.

With the lines identified, the vertices of each photovoltaic module were located in the thermal images, as they correspond to the intersection points between the lines detected in the edge images. This step was essential for the accurate mapping of each module's contour.

Next, the projective transformation was inverted in order to recover the frontal (orthogonal) view of each photovoltaic module. This operation used the previously located vertices, in the same manner as in the methods described by Henry et al. (2020) and Menéndez et al. (2018).

At the end of the process, the frontal view of each photovoltaic module was saved as a new thermal image, resulting in a dataset of thermal images individualized by module. This entire process ensured spatial consistency among the analyzed modules, a fundamental requirement for the reliable application of thermal dissimilarity metrics.

2.4. Temperature estimation of each segmented photovoltaic module

To obtain the temperature matrix associated with each captured thermal image, the *DJI Thermal SDK*, a Software Development Kit (SDK) provided by the drone manufacturer, was used. The procedure for measuring the emissivity of some of the photovoltaic modules was conducted in accordance with the recommendations of the Brazilian standard (NBR, from the portuguese *Norma Brasileira*) 16969:2021, from the Brazilian Association of Technical Standards (ABNT, from the portuguese *Associação Brasileira de Normas Técnicas*), which establishes general principles for the application of the infrared thermography method (ABNT, 2021). Accurate emissivity measurement is critical for correctly interpreting thermal images of photovoltaic modules. Figure 5 shows the experimental setup used for measuring the emissivity on the module surfaces.

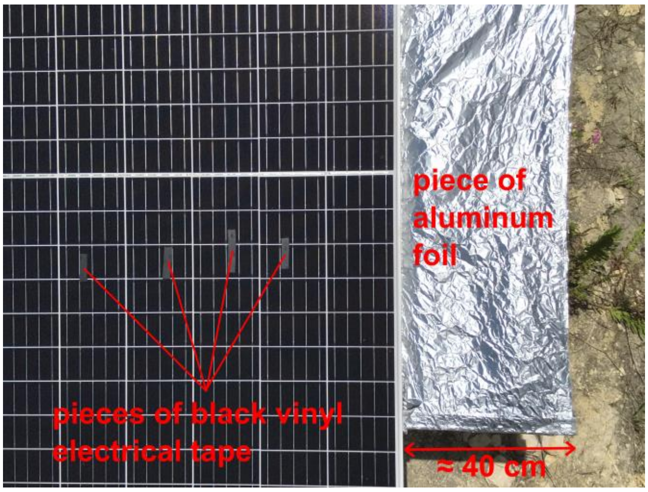

Figure 5: Experimental setup for measuring the emissivity on the surface of photovoltaic modules.

2.5. Dissimilarity measurement between temperature matrices of thermal images of photovoltaic modules

The main step of the analysis consisted of quantifying the thermal dissimilarity between photovoltaic modules, aiming to detect anomalous temperature variations associated with potential hotspots. The metrics used for comparing the temperature matrices of two thermal images, X and Y, were the sum of absolute differences — also known as the L1 norm or Manhattan norm — as represented in equation 2, and the squared Euclidean distance — also called the square L2 norm — as represented in equation 3.

$$SAD(X,Y) = \sum_{i=1}^{n} |x_i - y_i| \qquad \text{(eq. 2)}$$

$$SSD(X,Y) = \sum_{i=1}^{n}\left(x_i - y_i\right)^2 \quad \text{(eq. 3)}$$

where x_i is an element of the temperature matrix X, with n elements, and y_i is the corresponding element of the matrix Y, also with n elements.

Initially, a reference set was established from photovoltaic modules considered free of thermal anomalies — that is, with a homogeneous temperature distribution and absence of hotspots. SAD or SSD values exceeding a previously defined threshold (T_{SAD} or T_{SSD}, respectively) were interpreted as indications of potentially defective modules. This threshold was defined empirically based on the statistical analysis of the dissimilarity value distribution, considering one standard deviation above the mean of the healthy modules.

3. Results and discussion

3.1. Analysis of the acquired thermal images

Figure 6 presents the thermal images of four photovoltaic modules segmented from a single photograph of a photovoltaic panel from the solar power plant. The image on the left (Figure 6a) corresponds to a module without hotspots, used as a reference for the subsequent analyses. The next image (Figure 6b) also represents a hotspot-free module. The remaining images (Figures 6c and 6d) correspond to modules intentionally subjected to shaded areas in order to induce the formation of hotspots.

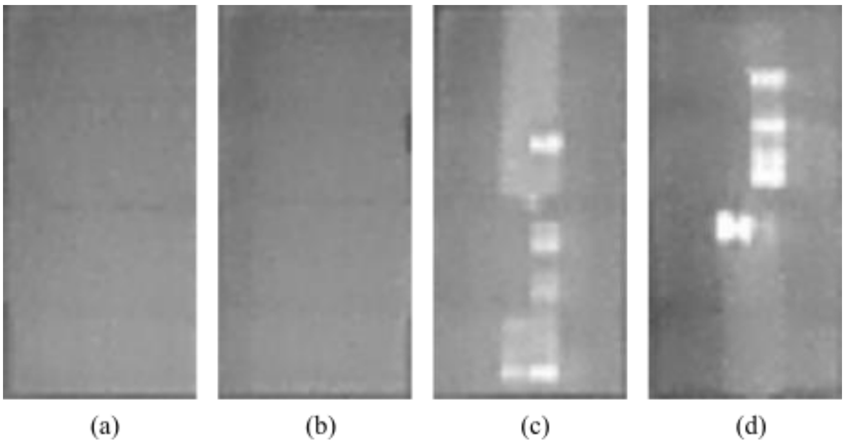

Figure 6: Four photovoltaic modules segmented from a single photograph of a panel.

The segmentation with projective correction enabled the acquisition of individualized thermal images for each module, allowing a detailed analysis of the thermal distribution and visual identification of hotspots.

3.2. Quantitative evaluation of thermal dissimilarity

Table 1 presents the dissimilarity measurement values between the reference photovoltaic module (Figure 6a) and the other analyzed modules, calculated using the SAD and SSD metrics.

Table 1: Dissimilarity measurements between the reference photovoltaic module and the other analyzed modules.

Dissimilarity between "a" and "b"	Dissimilarity between "a" and "c"	Dissimilarity between "a" and "d"
$SAD(a,b) \approx 354$	$SAD(a,c) \approx 14296$	$SAD(a,d) \approx 81738$
$SSD(a,b) \approx 613$	$SSD(a,c) \approx 99363$	$SSD(a,d) \approx 3087800$

It can be observed that the dissimilarity measurements are higher in the photovoltaic module exhibiting the largest number of hotspots (Figure 6d), indicating greater thermal variation compared to the reference module. Conversely, the module without visible hotspots (Figure 6b) showed considerably lower dissimilarity values, close to those expected for healthy modules.

These results corroborate the effectiveness of the SAD and SSD metrics for the quantitative detection of thermal anomalies, enabling a clear distinction between normal photovoltaic modules and those with potential defects.

4. Conclusions

In this work, the evaluation of hotspots in photovoltaic modules of a solar power plant was carried out through the measurement of dissimilarity between temperature matrices of thermal images acquired by drone. The adopted method combined precise module segmentation, the acquisition of temperature matrices using the thermal camera SDK, and the application of the SAD and SSD metrics for the quantification of thermal anomalies.

The results demonstrated that the dissimilarity metrics are effective in identifying thermal anomalies, particularly highlighting their ability to distinguish normal photovoltaic modules from those with potential thermal defects. The drone-based approach proved suitable for large-scale aerial inspections, ensuring both quality and safety in data collection. Thus, this work contributes to the advancement of predictive maintenance practices in photovoltaic systems, aligning with the trends and challenges discussed at the Solar World Congress 2025, which emphasizes technological innovation and sustainability in the solar sector.

Future work may explore the full automation of the segmentation and analysis process, as well as the application of machine learning algorithms to enhance the detection and classification of faults in photovoltaic systems.

5. Acknowledgments

The authors would like to thank the *Grupo Sergipe de Comunicação* for granting authorization and support for carrying out this research at their photovoltaic solar power plant. Their collaboration was essential for conducting the thermal inspections and for the development of this study. The authors also acknowledge CAPES and FAPITEC/SE for providing funding to attend the Solar World Congress 2025.

6. References

Associação Brasileira de Normas Técnicas, 2021. ABNT NBR 16969: Ensaios não destrutivos – termografia infravermelha – princípios gerais. 1st. ed. ABNT.

Duda, R.O., Hart, P.E., 1972. Use of the Hough transformation to detect lines and curves in pictures. Communications of the Association for Computing Machinery (ACM). 15, 11-15.

Henry, C., Poudel, S., Lee, S.-W., Jeong, H., 2020. Automatic detection system of deteriorated PV modules using drone with thermal camera. Applied Sciences. 10, 3802-3817.

International Electrotechnical Commission, 2017. IEC TS 62446-3: Photovoltaic (PV) systems – requirements for testing, documentation and maintenance – part 3: photovoltaic modules and plants – outdoor infrared thermography. 1st. ed. IEC.

Ikejiofor, O.E., Asuamah, Y.E., Njoku, H.O., Enibe, S.O., 2020. Detection of hotspots and performance deteriotations in PV modules under partial shading conditions using infrared thermography. Engineering Proceedings. 2, 71-77.

Menéndez, O., Guamán, R., Pérez, M., Cheein, F.A., 2018. Photovoltaic modules diagnosis using artificial vision techniques for artifact minimization. Energies. 11, 1688-1710.

Zhang, P., Zhang, L., Wu, T., Zhang, H., Sun, X., 2017. Detection and location of fouling on photovoltaic panels using a drone-mounted infrared thermography system. Journal of Applied Remote Sensing. 11, 16026-16036.